Journal of New Technology and Materials (JNTM)
J. New Technol. Mater.
Vol. 12, N°02 (2022)62-69

OEB Univ. Publish. Co.

First-principles investigation of magneto-electronic properties and band Jahn-Teller effects in $NiCoMnSi_{1-x}Al_x$ quaternary Heusler

E. H. Abbes[a,b,*], H. Abbassa[a,b], S. Meskine[a], I. Bouhamou[a,b] and A. Boukortt[a]

[a]*Elaboration and Characterization Physical Mechanics and Metallurgical of Materials Laboratory (ECP3M) Faculty of science and technology, Electrical Engineering Department,Abdelhamid Ibn Badis University-Mostaganem, Route nationale N°11, Kharrouba, 27000 Mostaganem, Algeria.*
[b]*Department of Physics, Faculty of Exact Sciences and Computer Science – Mostaganem, Algeria.*

*Corresponding author, email: habib.abbes.etu@univ-mosta.dz

Received date: Sep. 1, 2022 ; accepted date: Nov. 4, 2022

Abstract

Using ab initio calculations, density functional theory (DFT) calculations have been performed to investigate the electronic and magnetic properties of $NiCoMnSi_{1-x}Al_x$ (x=0, 0.25, 0.50, 0.75 and 1) quaternary Heusler compounds. To check the evolution of band Jahn teller effect in quaternary Heusler alloy and known the main raison to get the ground state energy by deforming the martensitic phase, we focused our work on the structural stability related to the formation of a Heusler alloy from two different crystallographic structures (cubic and tetragonal), for different concentrations. The structural, electronic and magnetic properties are calculated for all concentrations in both cubic and tetragonally distorted structure. Variation of total energy versus volume indicates that the crystallographic structures shift the cubic shape from a concentration of 0.50, which can be essential due to the Jahn-Teller effect. Magnetic properties of all studied alloys give the total magnetic moment of 4.086 μ_B, 4.561 μ_B, 5.024 μ_B, 5.092 μ_B and 5.000 μ_B respectively. With an integer value of total magnetic moment, NiCoMnAl alloy has a 100% spin polarisation at Fermi level with a half-metallic behaviour.

Keywords: ab-initio calculations ; Band Jahn-Teller effect ; ferromagnetic ; Heusler compounds.

1. Introduction

The equiatomic quaternary Heusler (EQH) compounds under the chemical formula XX'YZ [1,2] constitute an important part among the Heusler compounds, they are derived from $CuHg_2Ti$-type structure (X_2YZ) when X atoms are different [3], X, X' and Y are transition metals, while Z is an *sp*-element [4,5], its crystallographic structure is often cubic, known as Y-type (Prototype LiMgPdSn) [6,7], it results from four interpenetrating sub-lattices (fcc) [8] with the space group $F\bar{4}3m$. Generally, there are three types of atomic arrangement [9], where type-I is often the most stable whose X, X', Y and Z elements are placed in 4c (1/4,1/4,1/4), 4d (3/4,3/4,3/4), 4b (1/2,1/2,1/2) and 4a (0,0,0) positions, respectively.

Recently, some tetragonal EQH alloys are found to be more stable comparative to their cubic structure by distorted the z axis. The tetragonal structure form a lower energy system due to the Jahn-teller effect. Elongation and compression of the z axis mean that the *c/a* ratio in the tetragonal distortion is greater or lower than 1, depending on the type of element and ligands in the octahedral complex. Motivating by these properties, we have investigated two EQH with varying Z element. Basing on structural and electronic calculations of NiCoMnSi, NiCoMnAl and their alloys, we give a detailed explanation of the origin of the tetragonal distortion in EQH, and we explain why NiCoMnSi and $NiCoMnSi_{0.75}Al_{0.25}$ are more susceptible to a distortion by presenting and comparing their PDOS in both cubic and tetragonal structure.

2. Computational Method

Our theoretical investigation was based on the self-consistent full potential linearized augmented plane wave (FP-LAPW) method in order to calculate the electronic structures [10], this method is implemented in WIEN2K code [11]. The Perdewe-Burkee-Ernzerhof generalised gradient approximation (GGA) [12,13] have been used as exchange-correlation correction, whose the space is divided into non-overlapping muffin-tin (MT) spheres, isolated by an interstitial region. Inside area in the muffin-tin sphere, basis functions are expanded as spherical harmonic functions, and Fourier series for interstitial region. In the present work, muffin-tin sphere radii are 2.20 a.u. for Ni, Co, and Mn, 1.90 a.u. for Si, 1.80 a.u. for Al. The cut-off parameter RmtKmax is taken as 9. As Gmax parameter (the largest vector in charge density Fourier expansion), we used 12. In order to separate the valence and core states, cut-off energy was chosen as −6 Ry. The convergence criteria that control energy and charge were selected as 0.0001Ry and 0.001e respectively for all self-consistency cycles. To construct the charge density in self-consistency step, we used the tetrahedron method [11] with a 104 special k points (for cubic structure) and 240 special k points (for tetragonal

structure) in the irreducible wedge (3000 k-points in the full Brillouin zone).

3. Results and Discussion

3.1. Structural properties

The equiatomic quaternary Heusler (EQH) compounds can crystallise in three ordinary cubic structures (Y-type) [14,15] according to the possible arrangements, and as it known at the literature, the type I often found to be more favourable of the most EQH. First step of our calculation is found which type presents the ground state energy for $NiCoMnSi_{1-x}Al_x$ (x=0, 0.25, 0.50, 0.75 and 1) compounds, for this, we have calculated and plotted the variation of energy versus volume for only NiCoMnSi alloy in fig. 1.a, from this figure, we confirmed the literature result above, where type-I corresponds to the ground state, taking into account the magnetic order, fig. 1.b shows that the ferromagnetic phase is more stable than the paramagnetic (non-magnetic) phase in NiCoMnSi compound. Type I was found to be the most stable in the NiCoMnSi compound, so it is evident that it remains more stable with other compounds such as $NiCoMnSi_{1-x}Al_x$ (x= 0.25, 0.50, 0.75 and 1).

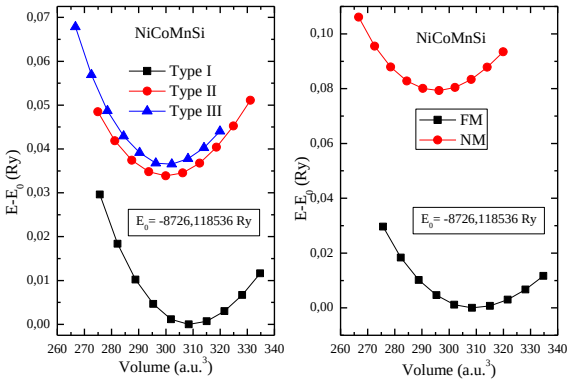

Figure 1. Difference in total energies ($E-E_0$) vs. volume for NiCoMnSi EQH: (a) the three types of atomic arrangement where E_0 represent the ground state energy in type I, (b) for ferromagnetic (FM) and paramagnetic (PM) order in type I.

Recent theoretical and experimental works [16-18] confirm the existence of a tetragonally distorted phase in EQH which crystallize in the cubic structure at 0 K temperature, generally due to the band Jahn-Teller effect [18]. Applying uniaxial distortion along the z axis, the cubic structure turns into a tetragonal structure with the space group $I\bar{4}m2$ where, Ni, Co, Mn and Z atoms are placed on the Wyckoff positions 2c (0,1/2,1/4), 2d (1/2,0,1/4) , 2b (0,0,1/2) and 2a (0,0,0), respectively.
To controlled the evolution of the Jahn teller effect and have more information about it, we have choose two compounds, one have this effect but the second have note, and we study the concentration between theme(x=0.25, 0.50 and 0.75) for the two possible structures. From the structural properties we have two method to testing the effect, once by calculate the variation of energy versus volume and know directly the more favorable structure or by the variation of the energy difference as a function of the distortion applied along the z axis, exactly at the value of $\sqrt{2} \approx 1.41$ coa ratio by having a peak or a valley, where the total energy takes the same value as well as that of the ground state in the cubic structure. Fig. 2. shows the structural optimization of the parent compounds NiCoMnAl and NiCoMnSi EQH . It is clear that tetragonal structure lowers the total energy and represents the ground state in NiCoMnSi alloy, but the NiCoMnAl alloy remains more stable in the martensitic structure (we can see that both cubic and tetragonal phases coincide). Fig. 3. shows the structural optimization of the all concentration compounds $NiCoMnSi_{1-x}Al_x$ (x=0.25, 0.50 and 0.75), It is clear that tetragonal structure lowers the total energy and represents the ground state only in 0.25 concentration.

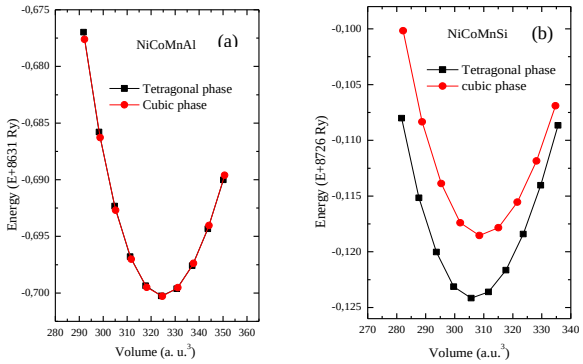

Figure 2. Total energy versus volume for (a) NiCoMnAl and (b) NiCoMnSi EQH.

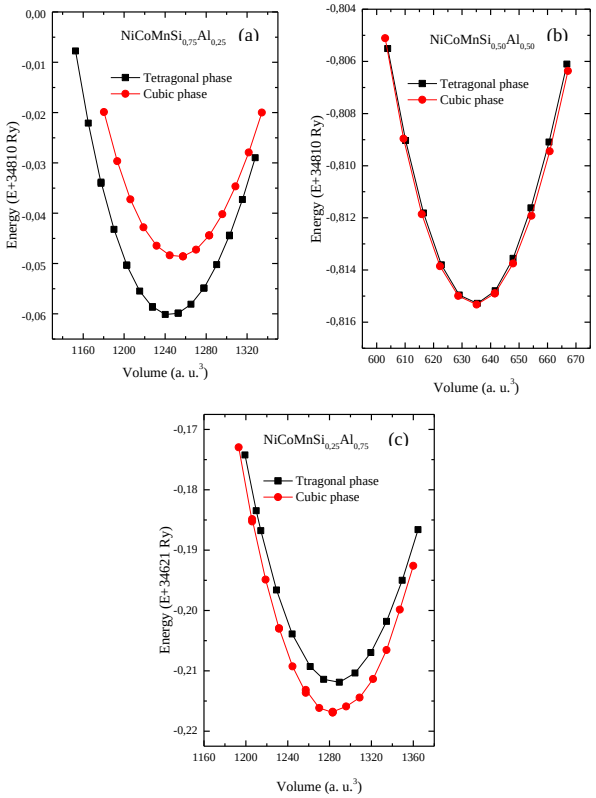

Figure 3. Total energy versus volume for (a) $NiCoMnSi_{0.75}Al_{0.25}$, (b) $NiCoMnSi_{0.50}Al_{0.50}$ and (c) $NiCoMnSi_{0.25}Al_{0.75}$EQH.

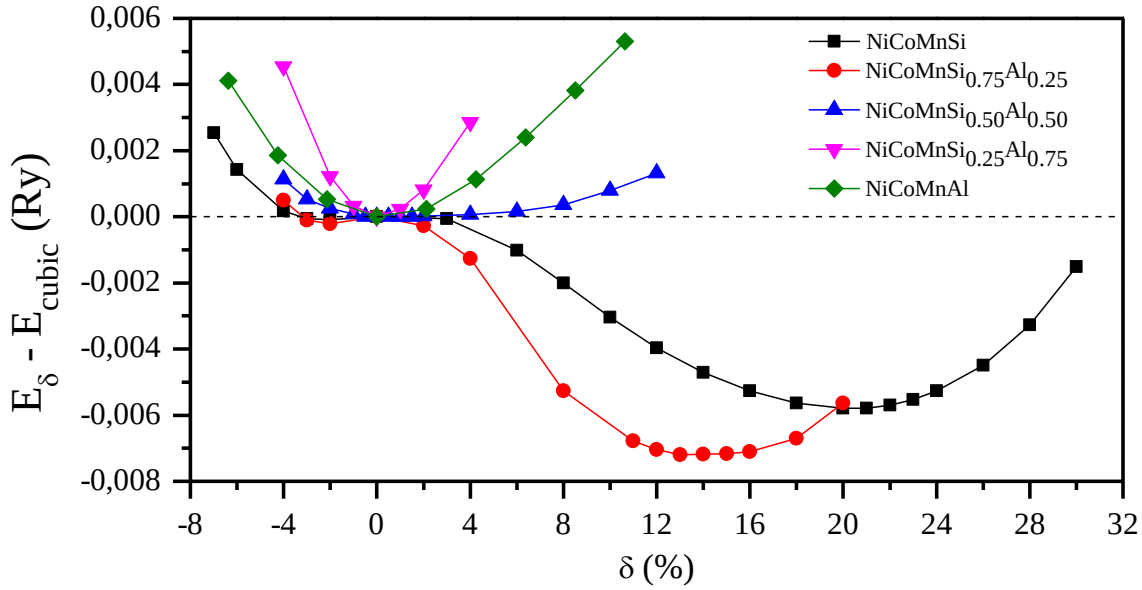

Figure 4. Total energy as a function of tetragonal strain along z-axis for $NiCoMnSi_{1-x}Al_x$ (x=0, 0.25, 0.50, 0.75 and 1) EQH.

This results are confirmed by the Fig. 4, this figure illustrates the variation of the energy difference (between tetragonally distorted and cubic phases) as a function of the distortion applied along the z axis, we notice that the resulting compound loses the tetragonal phase from a concentration of 0.50, which can be essential due to the non-existence of Jahn-Teller effect. It is clear that we have two minimums only on NiCoMnSi and $NiCoMnSi_{0.75}Al_{0.25}$ EQH contrary to the others compounds.

Basing on the non-linear fitting and using Murnaghan's equation (1) of states [19], we were able to determine the ground states properties for our studied compounds. The obtained results are listed in Table 1, in which we have cited some available results of the other works.

$$E(V) = E_0 + \frac{B}{B'(B'+1)}\left[V\left(\frac{V_0}{V}\right)^{B'} - V_0\right] + \frac{B}{B'}(V - V_0) \quad (1)$$

In order to confirm the possibility of realization of the parent compounds NiCoMnAl and NiCoMnSi EQH, we calculated the formation energy E_f using [2]:

$$E_f = E^{total}_{\mathrm{NiCoMnZ}} - (E^{bulk}_{Ni} + E^{bulk}_{\mathrm{Co}} + E^{bulk}_{\mathrm{Mn}} + E^{bulk}_{\mathrm{Z}}) \quad (2)$$

Where $E^{total}_{\mathrm{NiCoMnZ}}$ is the total energy of NiCoMnAl/NiCoMnSi per formula unit, and E^{bulk}_{Ni}, E^{bulk}_{Co}, E^{bulk}_{Mn} and E^{bulk}_{Z} are the total energies per atom of each element in the bulk for the Ni, Co, Mn, and Z, respectively. The negative formation energies (in Table 1) indicate the possibility of formation and the structural stability of these EQH compounds.

From Table 1, it is clear that our calculated lattice parameter a = 5.773 Å for NiCoMnAl is close to experimental value that indicated by Halder *et al* [9], 5.778 Å. for NiCoMnSi EQH, we did not find any experimental value in the literature.

Table1: Structural Parameters, the lattice parameter a in (Å), c/a ratio, Bulk modulus B in (GPa) and its first pressure derivative B' and formation energy in (eV) for $NiCoMnSi_{1-x}Al_x$ (x=0, 0.25, 0.50, 0.75 and 1) EQH.

$NiCoMnSi_{1-x}Al_x$	a (Å)	c/a	B_0 (GPa)	B'	E_f (eV)
NiCoMnSi	3.740	1.736	197.784	4.778	-2.255
Other Calc. [20]	3.738	1.737	198.592	4.920	
$NiCoMnSi_{0.75}Al_{0.25}$	3.851	1.615	189.618	4.784	-2.951
$NiCoMnSi_{0.50}Al_{0.50}$	5.730		173.253	4.568	-3.674
$NiCoMnSi_{0.25}Al_{0.75}$	5.750		167.921	4.702	-4.352
NiCoMnAl	5.773		170.936	4.322	-1.694
Other Calc. [21]	5.754				
Other Calc. [9]	5.778				

3.2. Electronic and magnetic properties

It is generally believed that one of the main reasons for a tetragonal distortion of EQH compounds is the DOS peaks near E_F [22-24] in the cubic phase. In order to investigate the origin of the band Jahn-Teller effect in EQH compounds and confirm the correlation of the high value of the DOS at E_F in the cubic phase, DOS (cub, E_F), with the probability of a tetragonal distortion, we calculated and plotted the band structure and the density of state in both cubic and tetragonal structures of NiCoMnSi and $NiCoMnSi_{0.75}Al_{0.25}$ EQH in Fig. 5,7 and Fig. 6,8 respectively, following the k-path for the band structure calculation as:

W - L - Γ - X - W - K

path for cubic structure (FCC lattice),

Γ - X - Y - Σ - Γ - Z - Σ_1 - N - P - Y_1 - Z

path for tetragonal structure (BCT_2 lattice), when c/a > 1 [25], R - Γ - X - M - Γ path for cubic supercell (no symmetry), and Γ- X - M - Γ -Z - R - A - Z path for tetragonal supercell (no symmetry)

Except for NiCoMnAl EQH, all studied alloys have a metallic ferromagnetic (MF) behaviour, with a spin polarisation less than 100% (Table 2).

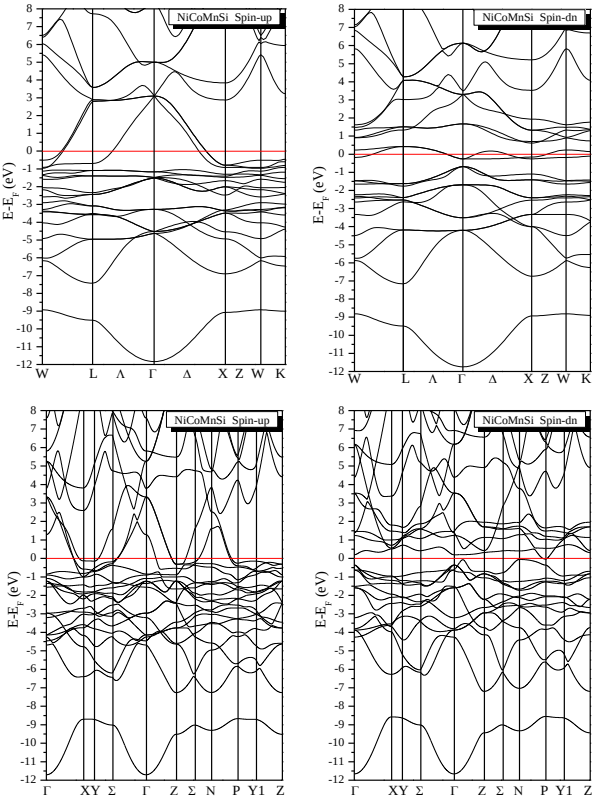

Figure 5. The calculated band structures of spin-up electrons (left panel), spin-down electrons (right panel) for NiCoMnSi EQH in the cubic phase (at the top) and the tetragonal phase (at the bottom).

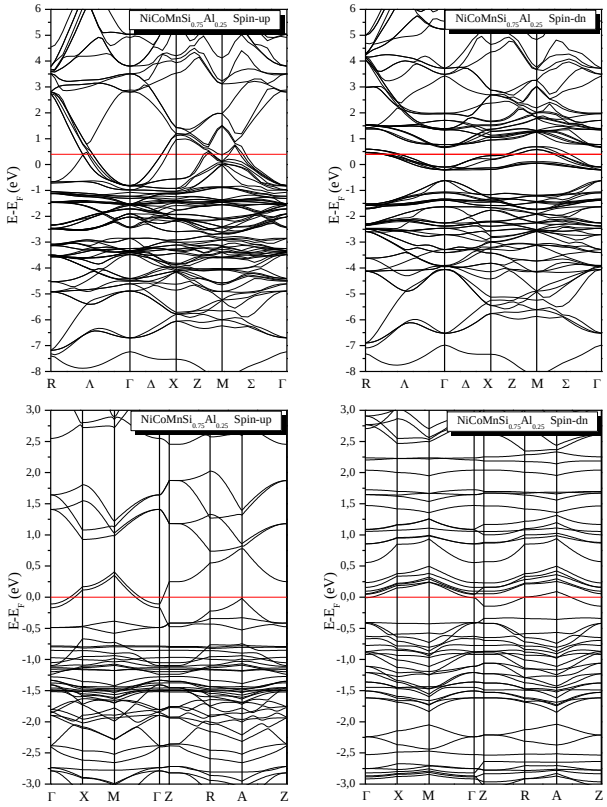

Figure 6. The calculated band structures of spin-up electrons (left panel), spin-down electrons (right panel) for NiCoMnSi$_{0.75}$Al$_{0.25}$ EQH in the cubic phase (at the top) and the tetragonal phase (at the bottom).

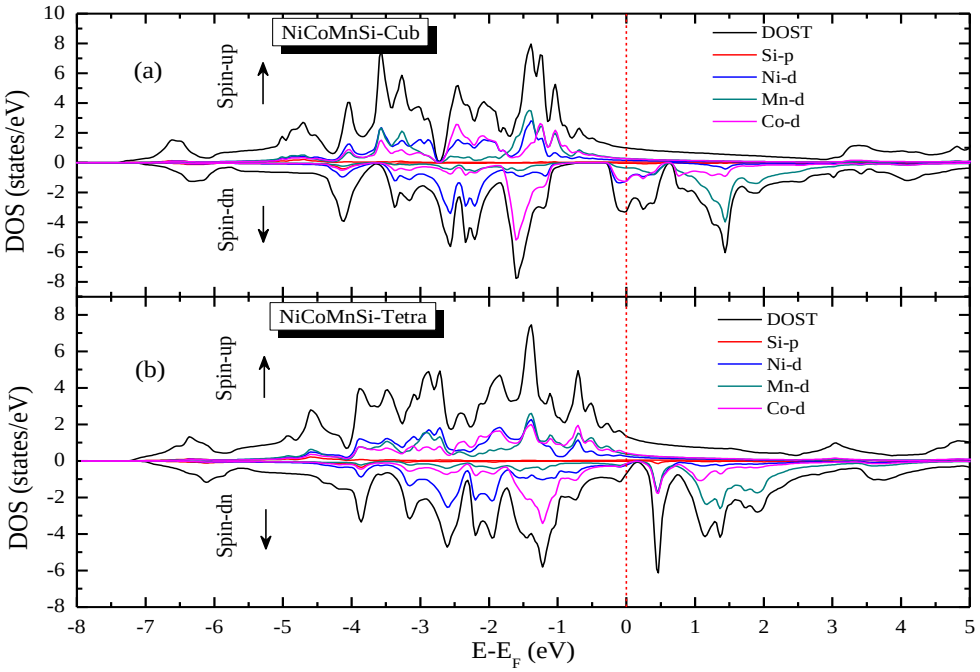

Figure 7. The calculated total/atomic projected densities of states of spin-up and spin-down electrons for NiCoMnSi EQH in the cubic phase (at the top) and the tetragonal phase (at the bottom).

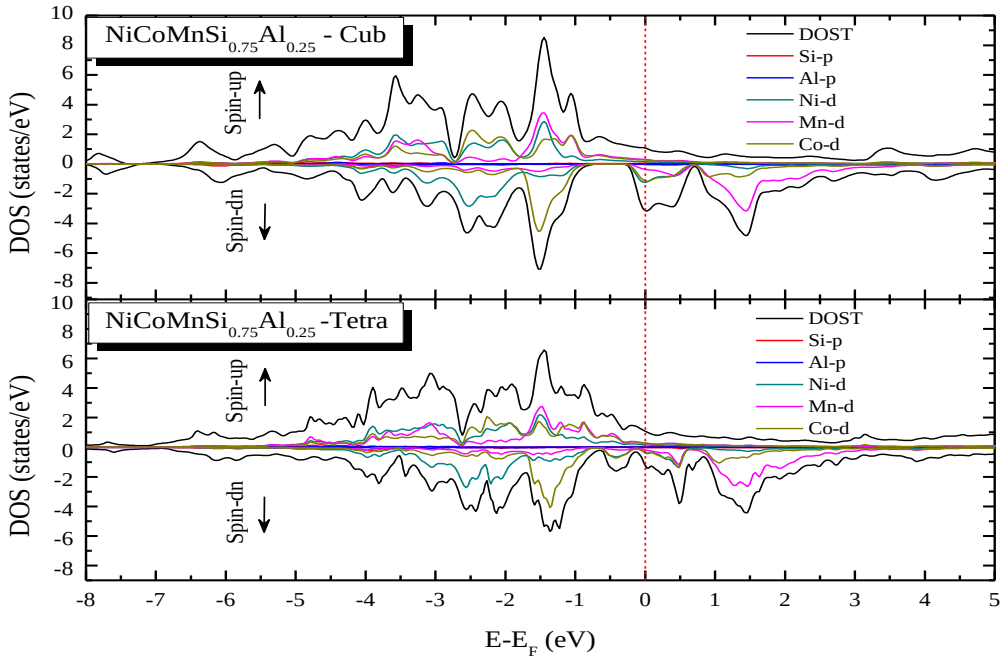

Figure 8. The calculated total/atomic projected densities of states of spin-up and spin-down electrons for $NiCoMnSi_{0.75}Al_{0.25}$ EQH in the cubic phase (at the top) and the tetragonal phase (at the bottom).

When E_F is in the middle of a DOS peak, the DOS(E_F) could be lowered by a tetragonal distortion [26] for several possible reasons [22,27,28].

Since one of the contributions to the total energy is the band energy [26]:

$$E_{band} = \int_{E_{min}}^{E_F} dEDOS(E)E \quad (3)$$

A reduction of the DOS near E_F in a tetragonal phase, in conjunction with conservation of the integral for the number of valence electrons (4), often leads to a lower band energy, and thus to a lower total energy for the tetragonal phase than for the cubic phase:

$$N_V = \int_{E_{min}}^{E_F} dEDOS(E) \quad (4)$$

Where E_{min} is the minimum energy of the valence bands.

From D.O.S (density of states) or band structure calculations, we clearly notice a metallic character at Fermi level in both spin-up and spin-down channel related to cubic and tetragonal structures for NiCoMnSi and $NiCoMnSi_{0.75}Al_{0.25}$ compound (Fig 5,6,7 and 8).

In the plotted density of states cubic phase, we notice a considerate peak at Fermi level for spin down channel in the density of state for NiCoMnSi (Fig.7.a) , and a very smooth shift (almost the same position) of this peak for $NiCoMnSi_{0.75}Al_{0.25}$ (Fig.8.a), whose the main contribution in D.O.S is due to Co and Ni atoms. Fig.7.b and Fig.8.b show a disappearance of the observed peak in the cubic structure, with the appearance of a strength peak just above Fermi level in corresponding tetragonal phase, where the major contribution is due to metals transition (Mn, Co, and Ni) for these two compounds.

The tetragonal distortion causes also a decrease in the spin polarisation, from 52.60% (cubic phase) to 31.85% (tetragonal phase) for NiCoMnSi, and from 49.64% (cubic phase) to 5.16% (tetragonal phase) for $NiCoMnSi_{0.75}Al_{0.25}$, it is completely related to the density of states calculation [29], where the main contribution is due to the *d* orbital of transition metals in all studied compounds.

Since cobalt is one of the most dominant elements in the peak located at Fermi level, we present its PDOS (partial density of states) in both cubic and tetragonal structures for NiCoMnSi and $NiCoMnSi_{0.75}Al_{0.25}$ EQH respectively. The peak in the minority DOS (Fig.9.a and Fig 10.a). (for spin down channel) at Fermi level E_F originates from the van Hove singularity associated with doubly degenerate eg bands at the Γ point [22] and is mainly due to e_g state of cobalt atom, where Co undergoes the octahedral field of Ni as e_g state is more energy than the t_{2g} state. The observed peak around 0.5 eV in the tetragonal distortion of NiCoMnSi and $NiCoMnSi_{0.75}Al_{0.25}$ (Fig.9.b and 10.b) leads to a splitting of these bands to d_{xy}, d_{xy} and d_{z^2} respectivement. Thus, the tetragonal distortion lowers the DOS(E_F), and thereby lowers the total energy of these compounds.

The calculated total and local magnetic moments and spin polarisation for $NiCoMnSi_{1-x}Al_x$ (x=0, 0.25, 0.50, 0.75 and 1) EQH alloys are listed in Table 2. We notice that the main contribution in the total magnetic in al studied compounds is due to manganese atom. Except for NiCoMnAl compound, non-integer values in total magnetic moments indicate a deviation from *Slater Pauling* behaviour [30] for other studied compounds.

$$M_{tot} = (Z_{tot} - 24)\mu_B \quad (5)$$

NiCoMnAl compound with integer value (5.000 μ_B) in total magnetic moment and nearly 100% spin polarisation is a nearly half metal (NHM) despite obedience to *Slater Pauling* rule. Fig. 11. show that Fermi level is just at the end of the band gap, this situation indicates a nearly half metallic (NHM) behaviour in nature for this compound.

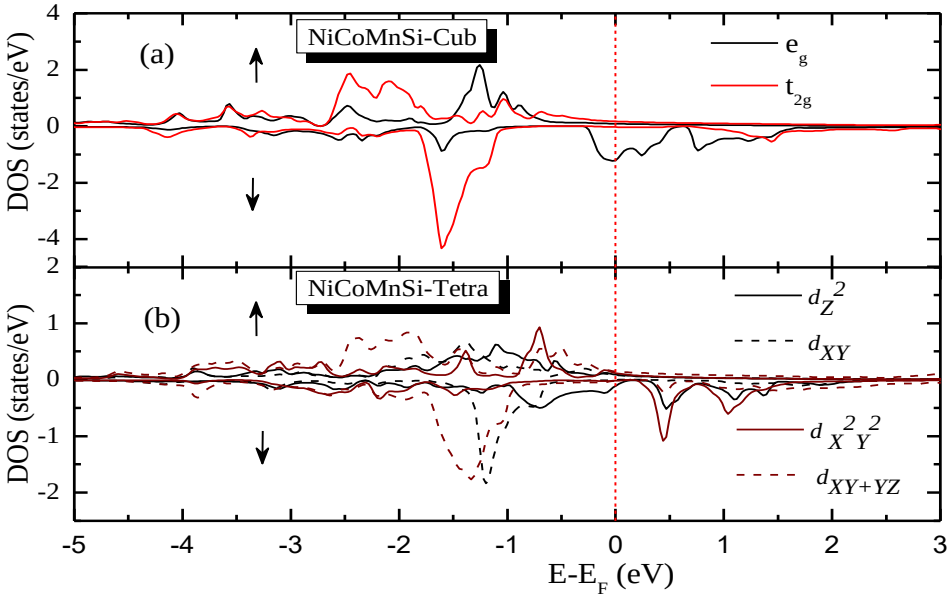

Figure 9. PDOS of 3*d*-Co orbital for (a) the cubic structure and (b) tetragonally distorted structure of NiCoMnSi.

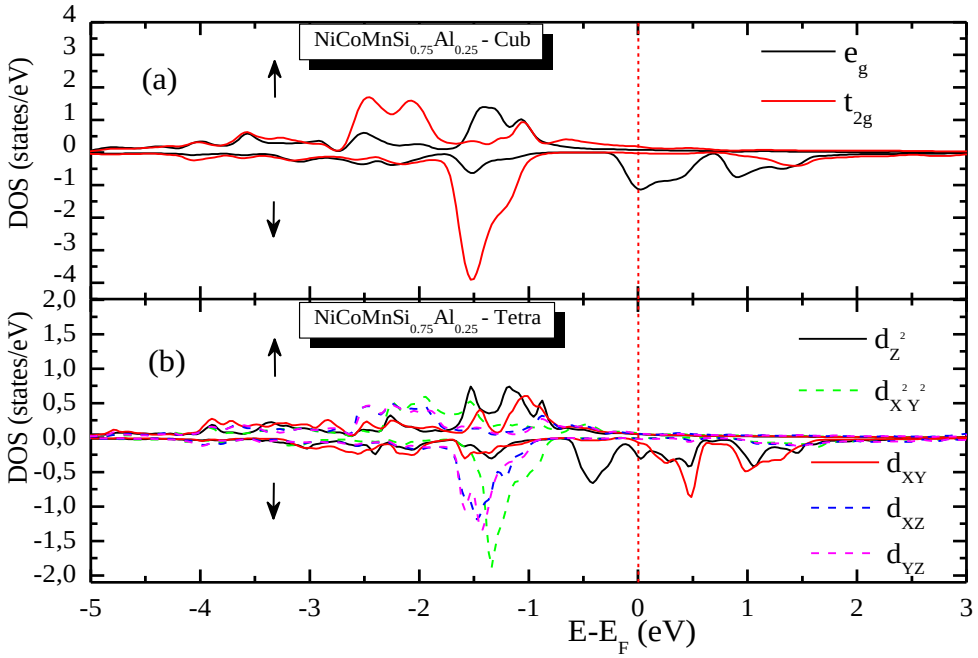

Figure 10: PDOS of 3*d*-Co orbital for (a) the cubic structure and (b) tetragonally distorted structure of $NiCoMnSi_{0.75}Al_{0.25}$.

Table2: Total and local magnetic moments per formula unit in (μ_B), and spin polarisation for $NiCoMnSi_{1-x}Al_x$ (x=0, 0.25, 0.50, 0.75 and 1) EQH.

$NiCoMnSi_{1-x}Al_x$	Total (/f.u)	Ni	Co	Mn	Al	Si	Interstitial	Spin pol. (%)
NiCoMnSi	4.086	0.357	0.813	2.968		-0.039	-0.013	31.85
Other Calc. [20]	4.080	0.356	0.811	2.965		-0.040	-0.012	34.41
$NiCoMnSi_{0.75}Al_{0.25}$	4.561	0.480	0.995	3.107	-0.025	-0.025	0.029	5.16
$NiCoMnSi_{0.50}Al_{0.50}$	5.024	0.595	1.219	3.215	-0.011	-0.021	0.027	46.54
$NiCoMnSi_{0.25}Al_{0.75}$	5.092	0.641	1.262	3.217	-0.013	-0.023	0.008	24.72
NiCoMnAl	5.000	0.643	1.250	3.183	-0.032		-0.044	nearly 100
Other Calc. [9].	5.00	0.63	1.25	3.24	-0.03		-0.079	

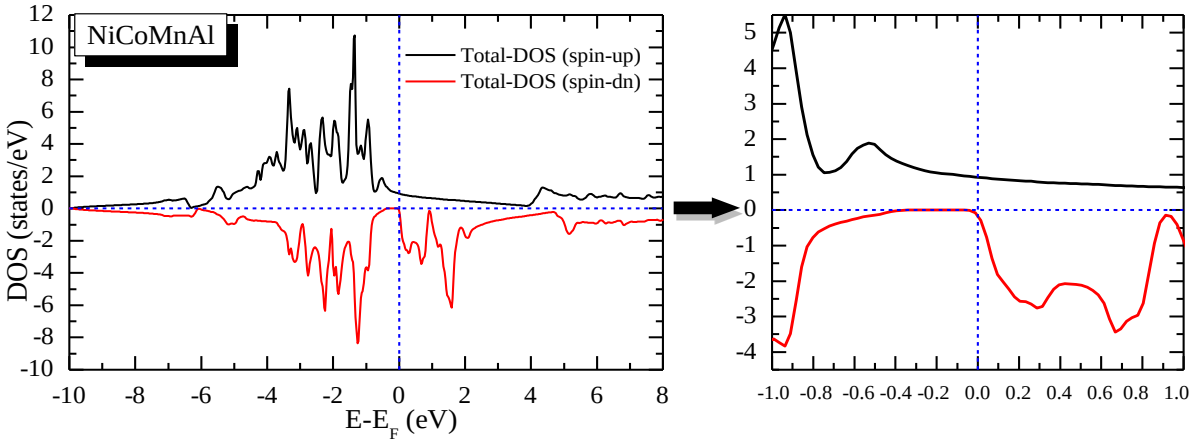

Figure 11. Total DOS of NiCoMnAl EQH at the ground state (cubic structure).

3.3. Elastic properties

The elastic properties play an important role to check the structural stability of the investigated compounds in the ground state. The elastic constants, Cij, determine the response of the crystal to external forces give more information for binding characteristic between adjacent atomic planes as well as structural stability, as characterized by the bulk, shear and Young's moduli and Poisson's ratio. Elasticity defines the characteristics of a solid material that undergoes stress, so deforms and recovers then returns to its original form after stress ceases [31].

Structural properties show that some of our compound crystallise in the cubic structure and other in tetragonal distortion. For tetragonal (tetragonal I) structure, it has six independent elastic constants such as: C_{11}, C_{12}, C_{13}, C_{33}, C_{44} and C_{66} (don't confuse with tetragonal-II structure which presents by symmetry seven independent constants C_{11}, C_{12}, C_{13}, C_{33}, C_{44}, C_{66} et $C_{16} = -C_{26}$ [32].). The cubic structure symmetry reduces elastic tensor elements to just three independent constants C_{11}, C_{12} and C_{44}.

To calculate this elastic constants for each structure from first principles we have two methods, one is related to the analysis of the calculated total energy of a crystal as a function of applied strain. The second one is based on the analysis of changes in the calculated stress values arising from variation in the strain. In our study, we choose the first method to predict the elastic constants. The degree of deformation of a crystal must be respected to a small strain δ of the lattice primitive cell volume V to remain within the yield point.

Using Taylor series expansions of the total energy, E(V,δ), The total energy variation as a function of applied strain can define the elastic constants C_{ij}, it can be expressed as [33]:

$$E(V,\delta) = E(V_0,0) + V_0\left(\sum_i \tau_i \xi_i \delta_i + \frac{1}{2}\sum_{ij} C_{ij}\delta_i\xi_i\delta_j\right) \quad (6)$$

Such as, $E(V_0,0)$ indicates the energy of the ground state with equilibrium volume V_0, τ_i is an element in the general stress tensor, and ξ_i is the factor characterizing the Voigt index.

We have calculated the elastic constants C_{ij} in each case basing Mehl Model [34-36]. (In both cubic and tetragonal structures according to the ground state structure).

The calculated elastic constants C_{ij} (for the ground state) are listed in Table 3. We call back that the elastic constants for cubic system should satisfy the following elastic stability criteria [37].

$$C_{11} > 0,\ C_{44} > 0,\ C_{11}-C_{12} > 0,\ C_{11}+2C_{12} > 0 \quad (7)$$

In the case of a tetragonal-I system, the elastic stability criteria are defined by [38,39].

$$C_{11} > 0,\ C_{33} > 0,\ C_{44} > 0,\ C_{66} > 0,\ C_{11}-C_{12} > 0,$$
$$C_{11}+C_{33}-2C_{13} > 0, \text{ and } [2(C_{11}+C_{12})+C_{33}+4C_{13}] > 0 \quad (8)$$

Table3: Calculated elastic constant C_{ij} (in GPa) for $NiCoMnSi_{1-x}Al_x$ (x=0, 0.25, 0.50, 0.75 and 1) EQH.

$NiCoMnSi_{1-x}Al_x$	C_{11}	C_{12}	C_{33}	C_{13}	C_{44}	C_{66}
NiCoMnSi	280.549	86.626	260.632	183.202	123.148	101.656
Other Calc. [20]	292.348	100.082	247.799	185.694	125.076	93.853
$NiCoMnSi_{0.75}Al_{0.25}$	309.012	54.944	243.290	189.319	142.797	99.398
$NiCoMnSi_{0.50}Al_{0.50}$	202.593	182.071			138.983	
$NiCoMnSi_{0.25}Al_{0.75}$	273.275	152.551			166.487	
NiCoMnAl	231.156	121.864			140.776	

From Table 3, it is clear that all elastic modulus check the criteria according to each structure. These results are in good agreement with those of Fig. 4, NiCoMnAl, $NiCoMnSi_{0.50}Al_{0.50}$ and $NiCoMnSi_{0.25}Al_{0.75}$ crystallize in the cubic structure, while NiCoMnSi and $NiCoMnSi_{0.75}Al_{0.25}$ crystallize in the tetragonal structure.

4. Conclusion

From electronic structure and magnetic properties of $NiCoMnSi_{1-x}Al_x$ (x=0, 0.25, 0.50, 0.75 and 1) EQH alloys investigated in this work, we conclude that:

Result of our calculations based on DFT, NiCoMnAl, $NiCoMnSi_{0.25}Al_{0.75}$ and $NiCoMnSi_{0.50}Al_{0.50}$ EQH alloys

crystallize in the cubic structure, while NiCoMnSi and $NiCoMnSi_{0.75}Al_{0.25}$ are affected by Jahn-Teller effect and crystallize in the tetragonal structure.
According to the elastic constant calculations, all structural stability criteria are satisfied for cubic and tetragonal structures, and confirm the formation energy calculations.
Except for NiCoMnAl, a non-integer value of total magnetic moment indicates that none of these Heusler compounds is a half metal.
The crystallographic structure obtained for a compound consisting of two materials with different structures, depends on their concentrations.

Acknowledgments
This work is supported by the Algerian national research projects, PRFU/DGRSDT/MESRS-Algeria (project N° B00L02UN270120220001).

References
[1] A. Birsan, *J. Alloy. Comp. 710* (2017) 393-398.
[2] Xiaotian Wang, Zhenxiang Cheng, Yaoxiang Jin, Yang Wu, Xuefang Dai, Guodong Liu, *J. Alloy. Comp. 734* (2018) 329-341.
[3] Hafsa Arshad, M. Zafar , S. Ahmad , M. Rizwan, M. I. Khan, S. S. A. Gillani , Chuan Bao Cao and M. Shakil, Mod. Phys. Lett. B (2019) 1950389.
[4] F. Heusler, *Verh. DPG* 1903, *5*, 219.
[5] Wei Zhang, Zhengnan Qian, Jinke Tang, Lei Zhao, Yu Sui, HongxiaWang, Yu Li, Wenhui Su, Ming Zhang, Zhuhong Liu, Guodong Liu and Guangheng Wu, J. Phys.: Condens. Matter *19* (2007) 096214 (8pp).
[6] A. İyigör and Ş. Uğur, Philosophical Magazine Letters *94* (2014) 708-715.
[7] Y. J. Zhang, Z. H. Liu, G. T. Li, X. Q. Ma, G. D. Liu, *J. Alloy. Comp. 616* (2014) 449.
[8] Lakhan Bainsla, A. K. Yadav, Y. Venkateswara, S. N. Jha, D. Bhattacharyya, K. G. Suresh, *J. Alloy. Comp. 651* (2015) 509-513.
[9] Madhumita Halder, M. D. Mukadam, K. G. Suresh, S. M. Yusuf, *J. Magn. Magn. Mater. 377* (2015) 220-225.
[10] D. J. Singh, "Planes waves, pseudo-potentials and the LAPW method", Kluwer Academic, Boston, 1994.
[11] Blaha P, Schwarz K, Madsen GHK, Hvasnicka D, Luitz J. Technische Universit Wien, ISBN 3-9501031-1-2; 2001.
[12] Perdew JP, Burke K, Wang Y, *Phys. Rev. B. 1996, 54*, 16533.
[13] Perdew JP, Burke K, Ernzerhof M, *Phys. Rev. Lett. 1996, 77*, 3865.
[14] Lakhan Bainsla, M. Manivel Raja, A. K. Nigam, K. G. Suresh, *J. Alloy. Comp. 651* (2015) 631-635.
[15] L. Zhang, X. Wang, Z. Cheng, *J. Alloy. Comp. 718* (2017) 63-74.
[16] Claudia Felser, Vajiheh Alijani, Jürgen Winterlik, Stanislav Chadov, and Ajaya K. Nayak, IEEE TRANSACTIONS ON MAGNETICS, VOL. *49*, No. 2, (2013) 682-685.
[17] J. Winterlik, S. Chadov, A. Gupta, V. Alijani, T. Gasi, K. Filsinger, B. Balke, G. Fecher, C. Jenkins, F. Casper, J. Kübler, G. Liu, L. Gao, S. Parkin, and C. Felser, *Advanced Materials, 24*, (2012) 6283-6287.
[18] Wenxu Zhang, Tao Yu, Zhishuo Huang and Wanli Zhang, *J. Alloy. Comp. 618* (2015) 78-83
[19] F. D. Murnaghan. *Proc. Natl. Acad. Sci. U S A 30* (1944) 5390.
[20] H. Abbassa, S. Meskine, A. Labdelli, S. Kacher, T. Belaroussi, B. Amrani, Materials Chemistry and Physics 256 (2020) 123735
[21] Jiangchao Han and Guoying Gao, *J. Phys. D: Appl. Phys.* 52 (2019) 505004
[22] J. Winterlik, S. Chadov, A. Gupta, V. Alijani, T. Gasi, K. Filsinger, B. Balke, G. H. Fecher, C. A. Jenkins, F. Casper, J. Kbler, G.-D. Liu, L. Gao, S. S. P. Parkin, and C. Felser, Adv. Mater. 24, 6283 (2012). [23] L. Wollmann, S. Chadov, J. Kübler, and C. Felser, Phys. Rev. B 92, 064417 (2015).
[24] Y.-I. Matsushita, G. Madjarova, J. K. Dewhurst, S. Shallcross, C. Felser, S. Sharma, and E. K. U. Gross, J. Phys. D. 50, 095002 (2017).
[25] W. Setyawan, S. Curtarolo, *Computational Materials Science 49* (2010) 299-312.
[26] S. V. Faleev, Y. Ferrante, J. Jeong, M. G. Samant, B. Jones, S. S. P. Parkin, Physical Review Applied, 7 (3), 034022 (2017).
[27] T. Graf, C. Felser, and S. S. P. Parkin, Prog. Solid State Chem. 39, 1 (2011).
[28] J. C. Suits, Solid State Commun. 18, 423 (1976).
[29] Benjamin Balke, Sabine Wurmehl, Gerhard H Fecher, Claudia Felser and Jürgen Kübler, Sci. Technol. Adv. Mater. 9 (2008) 014102
[30] A. Bahnes, A. Boukortt, H. Abbassa, D.E. Aimouch, R. Hayn, A. Zaoui , J. Alloys Compd. 731 (2018) 1208-1213.
[31] H. Rached, D. Rached, R. Khenata, Ali H. Reshak, and M. Rabah, *Phys. Status Solidi B 246*, No. 7 (2009).
[32] P.P. Gunaicha, S. Gangam, J.L. Roehl, S.V. Khare, Solar Energy 102 (2014) 276–281.
[33] L. Fast, J. M. Wills, B. Johansson, O. Rriksson, *Phys. Rev. B 51*, 17431 (1995).
[34] M. J. Mehl, J. E. Osburn, D. A. Papaconstantopoulos, and B. M. Klein, *Phys. Rev. B 41*, (1990) 10311.
[35] M. J. Mehl, *Phys. Rev. B 47*, (1993) 2493.
[36] M. J. Mehl, B. M. Klein, and D. A. Papaconstantopoulos, in: Principles Intermetallic Compounds, edited by J. H. West-Brook and R. L. Fleisher, Vol. 1 (Wiley, New York, 1995), chap.9.
[37] O. Baraka, S. Amari and A. Yakoubi, SPIN, Vol. 8, No. 3 (2018) 1850009
[38] Tarik Ouahrani, AlbertoOtero-de-la-Roza, A.H.Reshak, R.Khenata, H.I.Faraoun, B.Amrani, M. Mebrouki, Víctor Luaña, Physica B 405 (2010) 3658–3664
[39] Mirza H. K. Rubel, K. M. Hossain, S.K. Mitro, M. M. Rahaman, M.A. Hadi, A. K. M. A. Islam, Materials Today Communications, (2020) 100935.